Ordering in Thermally Oxidized Silicon

A. Munkholm* and S. Brennan†
Stanford Synchrotron Radiation Laboratory, Stanford Linear Accelerator Center, Menlo Park, California 94025, USA
(Received 29 January 2004; published 16 July 2004)

We present new evidence and a model for residual ordering of silicon atoms within the oxide of thermally oxidized silicon wafers. X-ray scattering is used to observe the residual order in thermally grown SiO_2 on Si(001), (011), and (111) surfaces with thicknesses of 60 to 1000 Å, for both on-axis and miscut surfaces. In every case, the scattering position can be predicted using a model which expands the silicon lattice during oxidation without completely disordering it. The amount of expansion and disorder is dependent on the type of oxidation process employed.

DOI: 10.1103/PhysRevLett.93.036106 PACS numbers: 68.55.Jk, 61.10.Eq, 81.05.Cy, 81.65.Mq

Despite decades of research on silicon and its oxide, there are still fundamental questions that remain unanswered about this technologically important materials system. It was not until the early 1990's that reports appeared of an epitaxial ordered oxide which extends throughout the thermal oxide [1,2]. These reports counter the wealth of studies that have concluded that the thermal oxide on silicon has no long-range order [3–5]. Ordering distributed throughout the SiO_2 film has been observed in thermal oxides but has not been found in deposited oxides [6] and has been observed for (001), (111) [7], and (011) [8] surfaces. There is general agreement that oxygen atoms diffuse through the silicon lattice and chemically react at the Si-SiO_2 interface [9–11]. This inward diffusion of oxygen into the silicon lattice results in an outward motion of the silicon atoms. Thermal oxides are fundamentally different from deposited oxides, where both silicon and oxygen atoms originate from gas-phase precursors.

In this Letter, we present a model which successfully predicts the ordered scattering observed with x rays. The model relies on the residual order of all of the silicon atoms in the oxide and does not require ordering of any of the oxygen atoms. Although the silicon atoms are translated towards the surface due to the injection of oxygen atoms and disordered by the oxidation process, the silicon atoms remain sufficiently ordered to scatter x rays at the lowest-order reflection of the new, expanded lattice. A single model applied to the (001), (011), and (111) surfaces with and without miscut successfully predicts the residual order peak positions. The model correctly predicts the shape of the scattering profile, which will be shown for the (001) surface. Although conceptually simple, the model we propose here can be used to understand the nature of the thermal oxidation process, especially near the Si-SiO_2 interface. Using our model to fit the scattered intensity, we are able to quantitatively obtain the density of the thermal oxide as a function of the distance from the interface.

To ensure that the observed scattering was not unique to one oxidation recipe, thermally oxidized silicon wafers were obtained from several integrated circuit manufacturers, and other wafers were oxidized at Stanford University. Both dry and wet oxidation processes were used, with oxide thicknesses ranging from 60 to 1000 Å. Here, data will be presented from a steam process 962 Å oxide on a Si(001) wafer with a 0.1° miscut (steam), as well as a 113 Å dry oxide Si(001) wafer with a 4° miscut along the [110] direction (miscut). A dry oxidation process at 1000 °C was used to produce 1000 Å thick oxides on (011) and (111) wafers.

Diffraction studies were performed at the Stanford Synchrotron Radiation Laboratory on beam line 7-2 with a four-circle diffractometer using a symmetric scattering geometry. Photons of 10 keV were focused by a toroidal mirror and passed by a Si(111) double crystal monochromator. Because of the miscut nature of many of the samples measured, the position of the crystal truncation rod (CTR) [12] was determined using an iterative procedure [13] at several out-of-plane values. After the CTR had been located, the profile of the enhanced scattering was measured by scanning along the CTR.

The scattering results from the steam sample are shown in Fig. 1 as dots, along with two theoretical predictions of the scattering. The model predicts the position of this residual order scattering peak by considering the change in atomic volume between bulk silicon (20.0 $Å^3$/Si-atom) and vitreous silica (44.5 $Å^3$/Si-atom). This ratio predicts the position of the diffraction peak from the residually ordered silicon, at 0.45 of the distance towards the *111* reflection, i.e., *1, 1, 0.45*. The scattering from the residual order coincides with the crystal truncation rod (CTR), which extends from the *111* bulk Bragg reflection towards the surface. The inset of Fig. 1 shows the range from the bulk reflection down to *1, 1, 0.3*, whereas the main figure shows only the region where the scattering from the residual order is observed. The intensity of the residual order scattering is 5 orders of magnitude less than the *111* intensity.

The model describes an expanded, disordered silicon lattice within the oxide in which the expansion and disorder are smallest at the interface and increase over a decay length to their far-field values. The lattice expansion along the surface normal is described by

 0031-9007/04/93(3)/036106(4)$22.50 © 2004 The American Physical Society

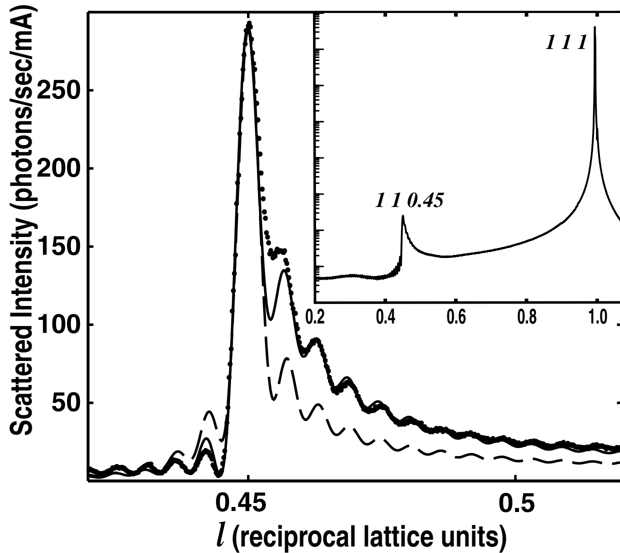

FIG. 1. Scattered intensity from a steam oxide on Si(001) is shown as dots. The solid line is the fit using an expansion of the silicon atoms which increases towards the surface, and the dashed line is the fit with a constant expansion throughout the oxide. The inset is the scattered intensity on a log scale along the entire 111 CTR, including the 111 Bragg peak.

$$\chi(z) = \chi_\infty + (\chi_0 - \chi_\infty) \exp\left(-\frac{z}{\tau}\right), \quad (1)$$

where χ_0 is the initial lattice expansion and χ_∞ is the lattice expansion far from the interface. The exponential increase of the expansion is over a characteristic length defined by τ. For a sample with zero miscut, the size of the expanded lattice at any position is $c(z) = a_0\chi(z)$, where a_0 is the bulk lattice parameter for silicon.

Static disorder of the silicon atoms in the oxide is described by a mean displacement u about their nominal position after expansion of the silicon lattice along the surface normal. The magnitude of the displacement is random for each atom and can be in any direction. The disorder increases as a function of distance z away from the Si-SiO_2 interface, defined by

$$u(z) = u_\infty + (u_0 - u_\infty) \exp\left(-\frac{z}{\tau}\right), \quad (2)$$

where u_0 is at the interface, followed by an exponential increase in disorder to a far-field value of u_∞. The characteristic distance τ is the same for both the lattice expansion and the disordering. Note that all the silicon atoms in the oxide are contributing to the observed scattering, but, due to their large static disorder, the scattered intensity is quite weak, as Fig. 1 inset shows. As the scattering is observed in a nonspecular direction, the silicon atoms in the oxide must have residual long-range order both parallel and perpendicular to the growth direction.

The calculation of the scattering from the substrate and the expanded silicon atoms within the oxide is based on a technique used to calculate crystal truncation rod scattering from any rational surface [14]. It includes the scattering amplitude from the substrate, from the ordered oxide film, and the cross term between the two. It is sufficiently general to be used for any surface orientation and is especially useful in calculating the scattering from miscut surfaces. The static disorder in the oxide is described using a standard Debye-Waller factor.

The solid line in Fig. 1 represents the calculated intensity using the model described above. The expansion of the lattice starts at $\chi_0 = 2.17$ at the interface and rises to $\chi_\infty = 2.23$ at the surface. The disorder at the interface is 1.02 Å, increasing to 1.65 Å at the surface. This value is quite large, as typical static disorder in crystalline metals is 0.1 Å, and may explain why the residual order has not been observed in transmission electron microscopy micrographs. The peak position is dominated by χ_∞; the extra intensity at $l > 0.45$ is due to a combination of the smaller expansion near the interface and the cross term between the scattering from the residual order and the scattering from the CTR. The dashed line in Fig. 1 uses the same parameters as the solid line, but with a constant $\chi = 2.22$ for the entire film. The fit to the data is significantly poorer, being much more symmetric than the data. The remaining asymmetry is due to the interference with the substrate CTR. If the interface were sufficiently rough, the CTR would not contribute to the scattering and the solid curve would be symmetric about the peak value. Thus any model proposed to explain the scattering which uses a crystalline oxide unit cell with a constant cell size throughout the film will not adequately fit the data. Thinner films will not show as strong an asymmetry as the data in Fig. 1, and some success has been achieved fitting such films with various crystalline oxide models [1]. Fits to the data were achieved using a genetic algorithm method [15] to minimize the difference between the data and the calculation. Error bars on the quoted values are ± 0.01 for the expansion, χ, ± 0.05 Å for the disorder, u, and ± 5 Å for the film thickness and characteristic length. Equation (1) can be used to determine the oxide density at any position within the oxide. Thus for the steam sample the density is 2.30 g/cm^3 at the interface, decreasing to 2.23 g/cm^3 at the surface. For comparison, bulk silicon is 2.33 g/cm^3. The higher silicon density at the interface is consistent with photoelectron spectroscopy studies that find evidence for suboxides at the Si-SiO_2 interface [16].

For a surface with a large miscut, the expansion is not along the crystallographic axis. Figure 2(a) shows the relationship between the substrate surface and the positions of the diffraction peaks from the expanded lattice. X-ray reflections from the silicon atoms in the expanded lattice have the same out-of-plane position with respect to the surface; therefore they are not at the same

out-of-plane position (l value) in bulk units. The constant expansion with respect to the surface is represented in Fig. 2(a) by the dashed line. The peak positions in Fig. 2(a) are specific to the data shown in Fig. 2(b), which are from the miscut sample. The peaks in bulk units are listed for each azimuth, being at $l = 0.37$ for the $-4°$ direction, $l = 0.47$ for the two azimuths with effectively no miscut, and at $l = 0.58$ for the $+4°$ direction. The position of the effectively 0° miscut azimuth constrains the values for the lattice expansion, and the positions of upper and lower peaks are constrained by the miscut. Thus the peak positions shown in Fig. 2(a) are specific to a particular sample, but the tilt of the CTR and the change in l position for different azimuths are true for any miscut angle.

In Fig. 2(b) the data are shown for the miscut sample. In the figure are three sets of data representing scattering along the $11l$ CTRs from the four $\langle 110 \rangle$ azimuths. The data from the $[1\bar{1}0]$ azimuth are identical to those from the $[\bar{1}10]$. Also shown in Fig. 2(b) as solid lines are the fits to those data. The fit was achieved for all three azimuths using the same values for χ_0 (2.17), χ_∞ (2.18), u_0 (1.23), u_∞ (1.62), τ (180 Å), miscut (4°), and film thickness (113 Å). One surprising characteristic of these data is the marked differences in intensity amongst the three peaks. Although the change in scattering vector q is

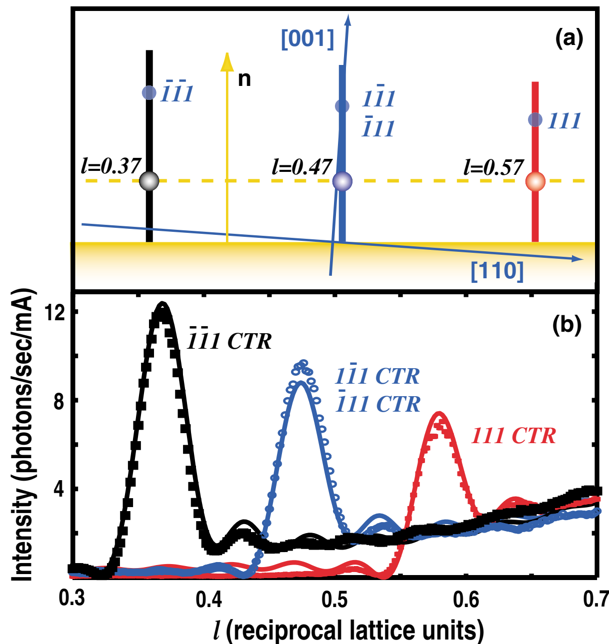

FIG. 2 (color). (a) Schematic of reciprocal space for a wafer with 4° miscut projected onto the $(\bar{1}10)$ plane. The streaks through the {111} Bragg peaks represent the crystal truncation rods shown in Fig. 2(b). The scattering from the oxide coincides with all CTRs and is positioned at a constant out-of-plane value from the surface. (b) Scattered intensity from the *111* CTR [red dots], $\bar{1}\bar{1}1$ CTR [black squares], and $1\bar{1}1$ and $\bar{1}11$ CTR [blue circles]. The solid lines represent the best fit to data.

<10%, the change in amplitude is nearly a factor of 2. That these data are successfully reproduced using a single set of parameters is further evidence for the validity of the model. The q dependence of the Debye-Waller factor is also the reason only the lowest order (*111*-like) reflections have been observed. All higher order reflections are too weak. For the steam sample, the peak from the *220* of the expanded lattice is calculated to be 1% of the *111* peak. Note that we are not identifying a subgroup of silicon atoms as being ordered. All the silicon atoms in the oxide contribute to the scattering based on their expanded lattice position along the surface normal and a Debye-Waller factor. Because the decay length τ for the miscut sample is longer than the film thickness, the expansion and the static disorder at the oxide surface are smaller than the far-field values (χ_∞ and u_∞).

Independent of the size of the miscut, the scattering from the ordered silicon coincides with the CTR from the underlying substrate. This is possible if the expanded lattice prior to disordering is coherent from step edge to step edge. This concept, shown in Fig. 3, results in a "pseudocell" where a is tilted both with respect to the silicon substrate and with respect to the surface plane, but c of this pseudocell is always aligned with the surface normal. Figure 3 presents these ideas as one possible set of silicon atomic positions in the oxide. For the sample in this study, the miscut is along the $\langle 110 \rangle$, hence the pseudocell is monoclinic, with $\alpha = \gamma = 90°$ and $\beta < 90°$. The figure is generated using the same procedures used to calculate the scattering profiles, with the specific fit parameters used for the data in Fig. 2(b). The oxygen positions are not shown in Fig. 3, nor are they considered in the calculation of the scattering. The miscut angle m of the bulk silicon lattice is 4° with respect to the $Si\text{-}SiO_2$ interface, which is shown in orange. The angle $m + \mu$ that the base of this unit cell forms with respect to the interface is determined by both the miscut size and the magnitude of the lattice expansion:

$$\tan(m + \mu) = \chi(z)\cos(m)\sin(m), \tag{3}$$

so the unit cell angle $\beta = 90 - (m + \mu)$. The in-plane lattice parameter of the pseudocell is given by

$$a(z) = a_0\sqrt{\frac{1}{2}[\chi^2(z)\sin^2(m) + 1/\cos^2(m)]}, \tag{4}$$

and the lattice parameter of the pseudocell along the surface normal is defined by

$$c(z) = \chi(z)a_0\cos(m). \tag{5}$$

Thus far, the model has successfully described the expansion of the silicon lattice for Si(001) surfaces with and without miscut; however, the model is equally successful in predicting the position of the expanded lattice scattering for the (011) and the (111) surfaces. The model uses the same principle of expanding the silicon lattice along

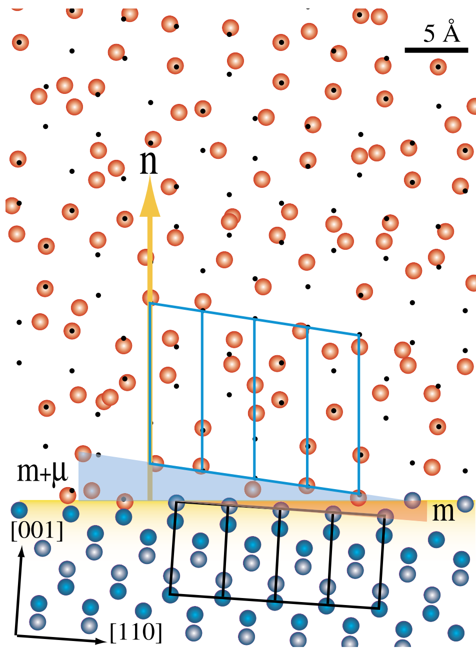

FIG. 3 (color). Illustration of the silicon positions near the Si-SiO_2 interface for a 4° miscut projected onto the ($\bar{1}10$) plane. The silicon atoms in the substrate are blue and those in the oxide are red. The small black spots represent the translated silicon positions in the absence of static disorder. The silicon atoms in the oxide have been randomly assigned a magnitude and direction based on the static disorder value at that position in the lattice. The outline of four silicon unit cells is shown in black, whereas the outline of four expanded lattice cells in the oxide is shown in blue.

the surface normal, an amount proportional to the change in silicon atomic volume. Thus, for the (011) surface, the positions of the residual order scattering are approximately at *1, 0.45, 0.45* and $\bar{1}$*, 0.45, 0.45*, i.e., less than $\frac{1}{2}$ way between the surface and the {111} reflections. For the (111) surface, there are four *111* reflections visible above the plane of the sample and thus four residual order peaks. There are three reflections of the type $\{-1.183, 0.817, 0.817\}$ and one reflection along the specular direction at *0.45, 0.45, 0.45*. Because the expansion is along the surface normal, the expanded lattice is very different for the different surface orientations. In each case, however, the model successfully predicts the position of the scattering from this expanded lattice. This is further evidence that the ordering is not due to a crystalline oxide which requires well-defined positions of both silicon and oxygen atoms. Measurements of the residual scattering on 1000 Å SiO_2 films on (011) and (111) surfaces agree with the predicted peak positions.

In summary, we have developed a model for the thermal oxidation of silicon which predicts the position and shape of extra diffraction peaks for any surface orientation. It is based on the indiffusion of oxygen which results in a translation of the silicon atoms towards the surface normal. Although this translation is associated with an increase in static disorder, the silicon atoms in the oxide remain sufficiently ordered to produce Bragg-like x-ray scattering from the oxide. The silicon residual order persists to the surface of the oxide even for ~1000 Å thick films, but the oxygen atoms are disordered throughout. Analysis of the scattering from this ordering results in several new insights into the nature of the thermal oxidation process: the amount of residual order in the oxide is dependent on the specific recipe used for the oxidation; the oxide is denser at the interface than at the surface, especially for thicker oxides; the interfacial oxide density is remarkably similar for all the samples in this study, despite a wide variety of thermal oxidation recipes; and analysis of the residual order peak can be used to determine the oxide density profile within the sample.

This research was carried out at the Stanford Synchrotron Radiation Laboratory, a national user facility operated by Stanford University on behalf of the U.S. Department of Energy, Office of Basic Energy Sciences.

After submission, similar results obtained by molecular dynamics simulations were published [17].

*Present address: Lumileds Lighting, San Jose, CA 95131, USA.
†Electronic address: sean.brennan@stanford.edu

[1] Y. Iida *et al.*, Surf. Sci. **258**, 235 (1991); I. Takahashi, T. Shimura, and J. Harada, J. Phys. Condens. Matter **5**, 6525 (1993).
[2] A. Munkholm *et al.*, Phys. Rev. Lett. **75**, 4254 (1995).
[3] N. F. Mott *et al.*, Philos. Mag. B **60**, 189 (1989).
[4] C. J. Sofield and A. M. Stoneham, Semicond. Sci. Technol. **10**, 215 (1995).
[5] W. Weber and M. Brox, MRS Bull. **12**, 36 (1993).
[6] T. Shimura, H. Sensui, and M. Umeno, Cryst. Res. Technol. **33**, 637 (1998).
[7] T. Shimura *et al.*, J. Cryst. Growth **166**, 786 (1996).
[8] T. Shimura *et al.*, in *The Physics and Chemistry of* SiO_2 *and the* Si-SiO_2 *Interface 3*, edited by H. Z. Massoud, E. H. Poindexter, and C. R. Helms (The Electrochemical Society, Pennington, NJ, 1996), p. 456.
[9] B. E. Deal and A. S. Grove, J. Appl. Phys. **36**, 3770 (1965).
[10] W. A. Tiller, J. Electrochem. Soc. **128**, 689 (1981); J. Electrochem. Soc. **130**, 501 (1983).
[11] Y. Tu and J. Tersoff, Phys. Rev. Lett. **84**, 4393 (2000); Phys. Rev. Lett. **89**, 086102 (2002).
[12] I. K. Robinson, Phys. Rev. B **36**, 3830 (1986).
[13] A. Munkholm and S. Brennan, J. Appl. Crystallogr. **32**, 143 (1999).
[14] T. P. Trainor, P. J. Eng, and I. K. Robinson, J. Appl. Crystallogr. **35**, 696 (2002).
[15] C. R. Houck, J. A. Joines, and M. G. Kay, "ACM Transactions on Mathematical Software" (to be published).
[16] F. J. Himpsel *et al.*, Phys. Rev. B **38**, 6084 (1988).
[17] K. Tatsumura *et al.*, Phys. Rev. B **69**, 085212 (2004).